Traffic patterns induced by the merging of two moving car platoons with different densities



2002 J. Phys. A: Math. Gen. 35 2145

(http://iopscience.iop.org/0305-4470/35/9/305)

INSTITUTE OF PHYSICS PUBLISHING JOURNAL OF PHYSICS A: MATHEMATICAL AND GENERAL

J. Phys. A: Math. Gen. **35** (2002) 2145–2157 PII: S0305-4470(02)30662-0

# Traffic patterns induced by the merging of two moving car platoons with different densities

**Rui Jiang and Qingsong Wu**

School of Engineering Science, University of Science and Technology of China, Hefei, 230026, People's Republic of China

E-mail: qswu@ustc.edu.cn

Received 7 November 2001, in final form 10 December 2001
Published 22 February 2002
Online at stacks.iop.org/JPhysA/35/2145

**Abstract**

In this paper, we investigate a common traffic phenomenon—the merging of a platoon of moving cars at one density into another platoon moving at a different density. A new macroscopic model, the 'speed gradient (SG) model,' is used in the simulations. It is shown that different traffic patterns appear according to different upstream and downstream densities. Generally, these patterns can be classified into stable traffic and unstable traffic. The transition from unstable pattern to stable pattern is discussed in detail.

PACS numbers: 45.70Vn, 89.40+k, 02.60Cb

## 1. Introduction

Over the last few decades, the development of various theories concerning traffic phenomena has received considerable attention [1, 2]. To understand the behaviour of traffic flow, various traffic flow models have been proposed and studied. Traditionally, two types are distinguished, i.e. microscopic models including car following [3–7] and cellular automaton models [8, 9] and macroscopic models including gas-kinetic [10–12] and hydrodynamic models [13–20].

Various traffic situations such as traffic bottleneck, narrow road sections, road gradients, on-ramps, off-ramps, lane closings etc [21–23] have been previously studied by both microscopic and macroscopic models. Three traffic states, i.e. free flow, traffic jam and synchronized traffic flow, are distinguished and analysed. The phase transitions among 'free flow $\longleftrightarrow$ synchronized traffic flow $\longleftrightarrow$ traffic jam' have been investigated. The obtained results are consistent with the experimental investigations [24, 25].

However, one common and fundamental phenomenon in traffic flow—the merging of a platoon of moving cars at one density into another platoon moving with a different density—has seldom been studied. This situation frequently appears in real traffic, as it may be caused by capacity reduction at bottlenecks and lane merging, the sudden change of speed of the

  

leading car of a uniform platoon of cars, and so on. It is important to know what transitions can possibly occur in the system to prevent instabilities and dangerous traffic situations.

Recently, Berg and Woods [26] have studied the situation using the optimal velocity (OV) model. They mainly dealt with the merging of two linear stable streams of cars of different densities and the traffic situations involving instability were not fully addressed.

Since unstable traffic always exists in real traffic, the motivation of this paper is to explore into the transition involving the unstable traffic. Compared to the microscopic models, macroscopic models are more suitable for real-time simulations; thus, we use the macroscopic simulations in this paper.

The paper is organized as follows. In section 2, we briefly introduce the macroscopic model used in the simulations. In section 3, we investigate the decelerating traffic, i.e. the transition from a low density to a high density. In section 4, we study the accelerating traffic, namely, the transition from a high density to a low density. The conclusion is given in section 5.

## 2. Traffic flow model

The development of macroscopic traffic flow models began with the LWR model presented by Lighthill and Whitham [13] and Richards [14]. Later other researchers proposed several high-order models [15–17]. However, there exist some problems in these high-order models, for example, characteristic speed and wrong way travel problem, etc [27].

Recently AW and Rascle [18] and independently, Jiang *et al* [19, 20] developed a new high-order macroscopic model for traffic flow. This new model comprises a continuum equation

$$\frac{\partial k}{\partial t} + \frac{\partial ku}{\partial x} = 0 \tag{1}$$

and a dynamics equation

$$\frac{\partial u}{\partial t} + u\frac{\partial u}{\partial x} = \frac{u_e(k) - u}{T} + c_0\frac{\partial u}{\partial x} \tag{2}$$

where $k$ is traffic density, $u$ is space mean speed, $x$ and $t$ denote space and time, respectively; $u_e(k)$ is an equilibrium relationship between the speed and the traffic density; $T$ is relaxation time and $c_0$ is propagation speed of disturbance. Equation (1) indicates that the number of vehicles on the road is in conservation. The left-hand side of (2) is the acceleration of vehicles. The first term on the right-hand side of (2) is a relaxation term, representing the process that drivers adjust the speed of the vehicles to equilibrium; the second term is an anticipation term, representing the process that drivers react to the traffic ahead.

In the new model, the anticipation term is represented by the speed gradient effect which differs from the density gradient effect in the previous models, and hereafter the new model is referred to as the speed gradient (SG) model. The two characteristic speeds of the SG model can be calculated as $\lambda_1 = u - c_0$ and $\lambda_2 = u$. It removes the problem that one characteristic speed is always greater than the macroscopic traffic speed $u$. Thus, it can embody the property that the vehicles are anisotropic and it does not exhibit the wrong way problem [27].

A linear stability analysis of the SG model [19] has found that the model is stable if $|ku'_e(k)| < c_0$. The maximum value of $|ku'_e(k)|$ is calculated to be 28.6 m s$^{-1}$ at $k =$ 0.041 vehicle m$^{-1}$, i.e. the model is always stable if $c_0 \geqslant 28.6$ m s$^{-1}$. Since we investigate the traffic involving instability, we need to choose $c_0$ that is smaller than 28.6 m s$^{-1}$.

In this paper, we use the SG model to simulate the proposed problem. Suppose $c_0 =$ const. and rewriting equations (1) and (2) in the conservation form, we have

$$U_t + F(U)_x = B(U) \tag{3}$$

where

$$U = \begin{pmatrix} k \\ u \end{pmatrix} \qquad F(U) = \begin{pmatrix} ku \\ \frac{1}{2}u^2 - c_0 u \end{pmatrix} \qquad B(U) = \begin{pmatrix} 0 \\ \frac{u_e(k)-u}{T} \end{pmatrix}.$$

We adopt an operator splitting with two steps [28] for equation (3) and split equation (3) into

$$U_t + F(U)_x = 0 \tag{4}$$
$$U_t = B(U). \tag{5}$$

Discretizing equation (4) by the HLLE scheme [29, 30], we have

$$U_{i,*}^{n+1} = U_i^n - \frac{\Delta t}{\Delta x}\left[F_{i+1/2} - F_{i-1/2}\right] \tag{6}$$

where $\Delta t$ and $\Delta x$ are the time and spatial intervals of discretization. The numerical flux $F_{i+1/2}$ is calculated by

$$F_{i+1/2} = \frac{a_R^+ F\left(U_i^n\right) - a_L^- F\left(U_{i+1}^n\right) + a_R^+ a_L^-\left(U_{i+1}^n - U_i^n\right)}{a_R^+ - a_L^-} \tag{7}$$

where $a_R^+ = \max(a_R, 0)$ and $a_L^- = \min(a_L, 0)$. $a_R$ and $a_L$ are numerical approximations for the largest and smallest physical signal velocities in the exact solution to the Riemann problem $\left(U_{i+1}^n, U_i^n\right)$:

$$a_R = \max\left(\frac{u_i^n + u_{i+1}^n}{2}, u_{i+1}^n\right) \qquad a_L = \min\left(\frac{u_i^n + u_{i+1}^n}{2} - c_0, u_i^n - c_0\right). \tag{8}$$

Taking the solution to equation (4) as the initial condition, we can numerically solve the ordinary differential equation (5). Since the HLLE scheme is only of first order, we can adopt the Euler backward difference for equation (5) whose precision matches the HLLE scheme. Thus, we have

$$U_i^{n+1} = U_{i,*}^{n+1} + \Delta t\, B\left(U_i^{n+1}\right). \tag{9}$$

Equations (6) and (9) constitute the numerical scheme for the SG model. The numerical stability of the scheme is guaranteed if the CFL condition

$$\max(|u|, |u - c_0|)\frac{\Delta t}{\Delta x} \leqslant 1$$

is met.

In the simulation, the equilibrium speed density function $u_e(k) = u_f(1 - k/k_j)\big/\left(1 + E(k/k_j)^4\right)$ proposed by Lee *et al* [21] is adopted, where $u_f = 33.3\ \mathrm{m\,s^{-1}}$ is the free flow speed, $k_j = 0.14$ vehicle $\mathrm{m^{-1}}$ is the jam density and $E = 100$. The fundamental diagram of flux against density from this equilibrium speed density function is shown in figure 1. Note that the chosen $u_e(k)$ function has a turning point, which is calculated to be $k_t = 0.047$ vehicle $\mathrm{m^{-1}}$ by setting $q''(k_t) = 0$ where $q(k) = ku_e(k)$.[1] In the simulation it is assumed that the relaxation time $T = 10$ s. The spatial interval $\Delta x = 100$ m and time interval $\Delta t = 2.5$ s are used for the discretization.

[1] In traditional traffic research [13], it is always required that the function should be concave because only under such a condition can it be guaranteed that no stationary acceleration wave occurs. It was previously believed that a stationary acceleration wave was unrealistic. However, recent experimental investigations [24] found that the stationary acceleration wave does exist in real traffic, such as the outflow from the wide jam. Moreover, recent research [31, 32] also pointed out that only a function with a turning point can render the kink–antikink density wave solution that represents the traffic jam. Thus, we choose the equilibrium speed density function with a turning point in this paper.

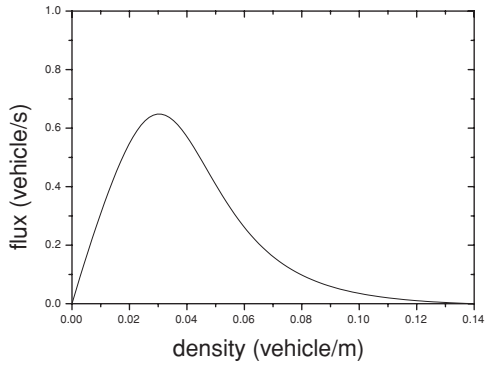


**Figure 1.** The fundamental diagram from Lee *et al*'s equilibrium speed density function.

## 3. Decelerating traffic

In this section, we explore the decelerating traffic (DT), i.e. the transition from a low density into a high density. In order to investigate the transitions between densities, we use the free boundary condition. That is, downstream boundary $k(x = L/2, t) = k(x = L/2 - \Delta x, t)$ and $u(x = L/2, t) = u(x = L/2 - \Delta x, t)$ and upstream boundary $k(x = -L/2, t) = k(x = -L/2 + \Delta x, t)$ and $u(x = -L/2, t) = u(x = -L/2 + \Delta x, t)$, where $L$ is the system size. The initial condition is $k = k_u, u = u_e(k_u)$ for $x \leqslant 0$ and $k = k_d, u = u_e(k_d)$ for $x > 0$.

First, we carry out the simulation at $c_0 = 20$ m s$^{-1}$. The simulations show that the DT can be either stable or unstable for different pairs of $(k_u, k_d)$. The stable DT can further be classified into six categories as shown in figure 2($a$). They are shock structure (region a), oscillatory (region b), Bando wave and a second stationary acceleration wave (region c), Bando wave, plateau and dispersive tail (region d), jump and dispersive tail (region e), and purely dispersive (region f). The representative patterns of the six regions are shown in figures 3($a$)–($f$) respectively. For regions c and d, the density first jumps from an upstream density $k_u$ to an intermediate density $k_b$, before it eventually matches the downstream density through a second stationary acceleration wave (region c) or dispersive tail (region d). The jump from the upstream density $k_u$ to the intermediate density $k_b$ is called the Bando wave, which is a shock in the DT case. The properties of the six stable patterns are analogous to those discussed in [26], thus in the following, we focus on the transition between the stable and unstable DT.

Since the unstable region g borders two different stable traffic regions b and c, we need to discuss the two situations separately. First, we consider the transition between regions g and c. If we fix the upstream density $k_u$ and merely change the downstream density $k_d$ near the boundary between regions c and g, we find that whether the traffic pattern is stable or not, the Bando wave is the same. The instability actually originates from the new accelerating traffic (AT) problem $(k_b, k_d)$. See figure 4 for the illustrated results. If the AT problem $(k_b, k_d)$ is stable, then the DT problem $(k_u, k_d)$ falls into the stable region c, as shown by the solid line. However, if the AT problem $(k_b, k_d)$ is unstable, then the DT problem $(k_u, k_d)$ becomes unstable traffic as shown by the dashed line. The stability of the AT problem will be discussed in section 4.

Next we consider the transition between regions g and b. Note that in the unstable region g, given the same downstream density, if the upstream density decreases to a certain value, then the instability disappears. For the purpose of explanation, we choose the following two typical downstream densities.

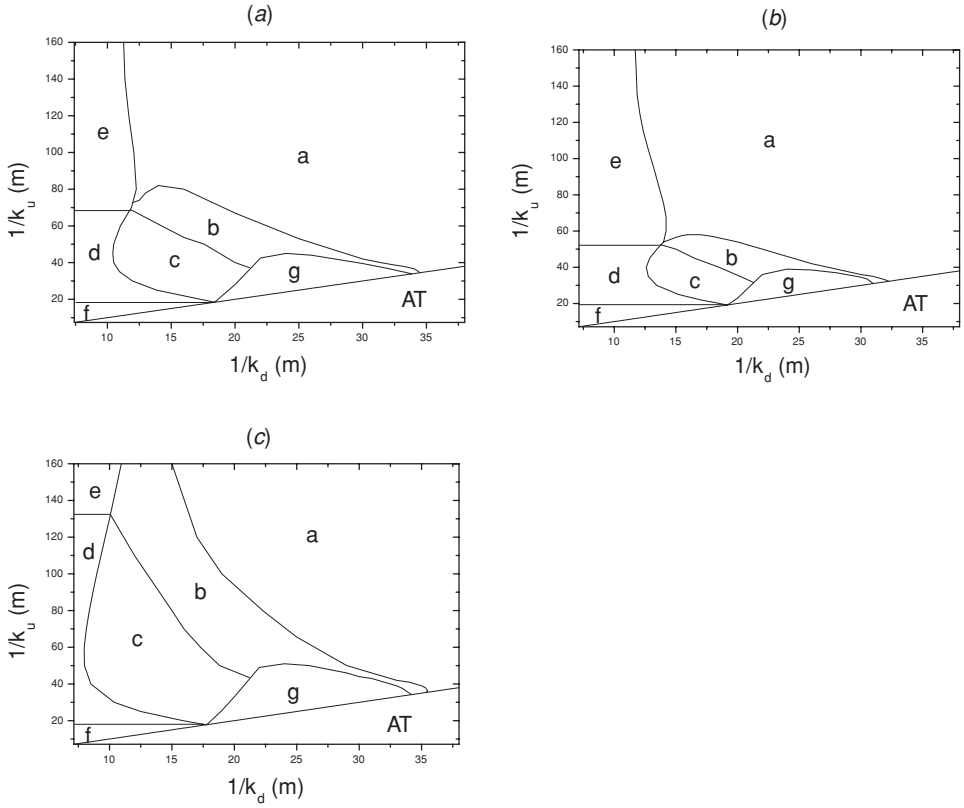


**Figure 2.** Transitions of the DT derived from the numerical simulations of the SG model at (*a*) $c_0 = 20$ m s$^{-1}$; (*b*) $c_0 = 22$ m s$^{-1}$; (*c*) $c_0 = 18$ m s$^{-1}$.

(i) $k_d = 0.030\,49$ vehicle m$^{-1}$. For such a downstream density, the unstable traffic is characterized by a single cluster (figure 5(*a*)). As pointed out by Kerner and co-workers [24, 33], the flow out of the cluster is the characteristic quantity of the traffic flow, which is independent of the initial conditions. With the decrease of the upstream density, the upstream flow rate decreases. If the upstream flow rate decreases to a value less than the characteristic outflow rate from the cluster, a cluster cannot be maintained even if it forms. Under this situation, oscillatory traffic exists instead of unstable traffic.

(ii) $k_d = 0.033\,33$ vehicle m$^{-1}$. The unstable traffic corresponding to this downstream density is characterized by complex sequences of clusters, which are self-generated repeatedly (figure 5(*b*)). For this case, even if the upstream flow rate is less than the characteristic outflow rate from the cluster, it does not always mean that the traffic is stable because if the dissolving rate of the cluster is not greater than the generating rate of the cluster, the clusters can still be maintained. For example, see the results presented in figure 6. We number the clusters in order to better understand the dissolving and generating of the clusters. We can see that from 4500 to 5000 s, one cluster 1 has been dissolved and two clusters 8 and 9 are generated. Only when the upstream flow rate is so small that the dissolving rate of the cluster is greater than the generating rate may the unstable traffic disappear.

Thus, we can conclude that the reason for the transition from region g to region b is that the upstream flow rate is not large enough to maintain the unstable traffic.

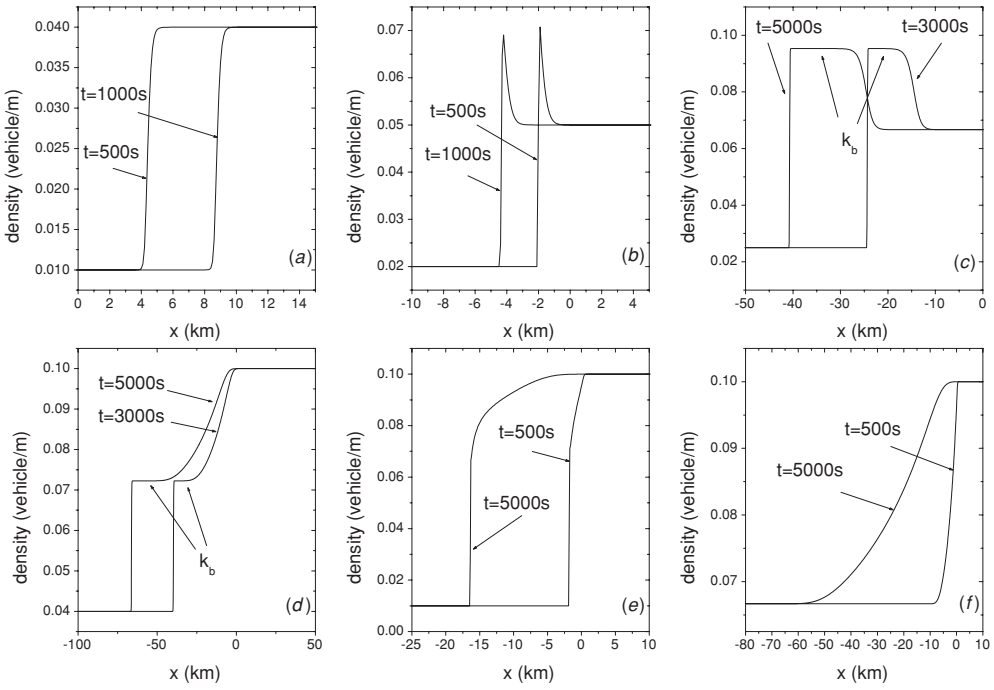


**Figure 3.** (*a*)–(*f*) The typical patterns of regions a–f in figure 2(*a*), where $k_u$ and $k_d$ are (*a*) 0.01, 0.04; (*b*) 0.02, 0.05; (*c*) 0.025, 0.066 67; (*d*) 0.04, 0.1; (*e*) 0.01, 0.1; (*f*) 0.066 67, 0.1 vehicle $m^{-1}$.

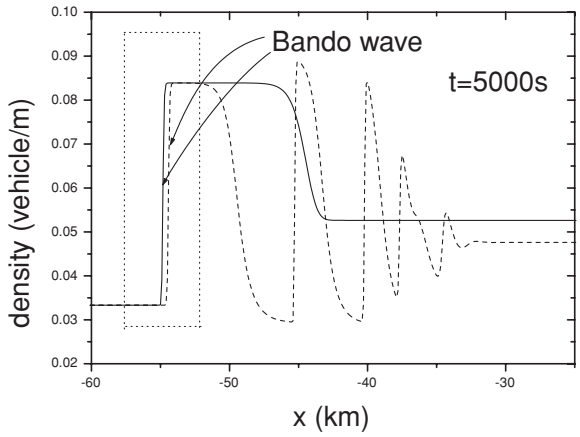


**Figure 4.** The two different traffic patterns near the boundary between regions c and g in figure 2(*a*). The solid line indicates the result of $k_u = 0.033\,33$ vehicle $m^{-1}$, $k_d = 0.052\,63$ vehicle $m^{-1}$, and the traffic pattern falls into region c. The dashed line indicates the result of $k_u = 0.033\,33$ vehicle $m^{-1}$, $k_d = 0.047\,62$ vehicle $m^{-1}$, and the traffic pattern falls into region g.

If we increase the value of $c_0$, the stability of the traffic flow is enhanced and accordingly the unstable region g shrinks. Meanwhile, regions b and c shrink as well. In contrast, regions a, d, e and f expand (figure 2(*b*)). Similarly, if we decrease $c_0$, regions b, c and g expand and

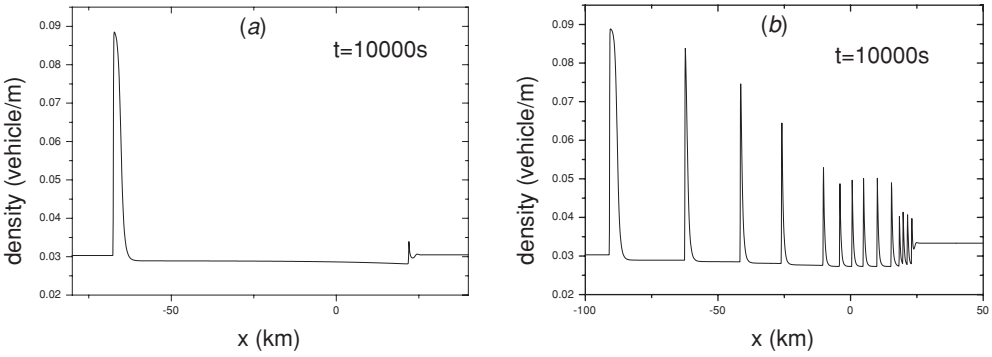


**Figure 5.** The different unstable traffic patterns of two typical downstream densities. (*a*) $k_d = 0.030\,49$ vehicle $\mathrm{m}^{-1}$, $k_u = 0.0303$ vehicle $\mathrm{m}^{-1}$, and the traffic pattern is characterized by a single cluster. (*b*) $k_d = 0.033\,33$ vehicle $\mathrm{m}^{-1}$, $k_u = 0.0303$ vehicle $\mathrm{m}^{-1}$, and the traffic pattern is characterized by a complex sequence of clusters.

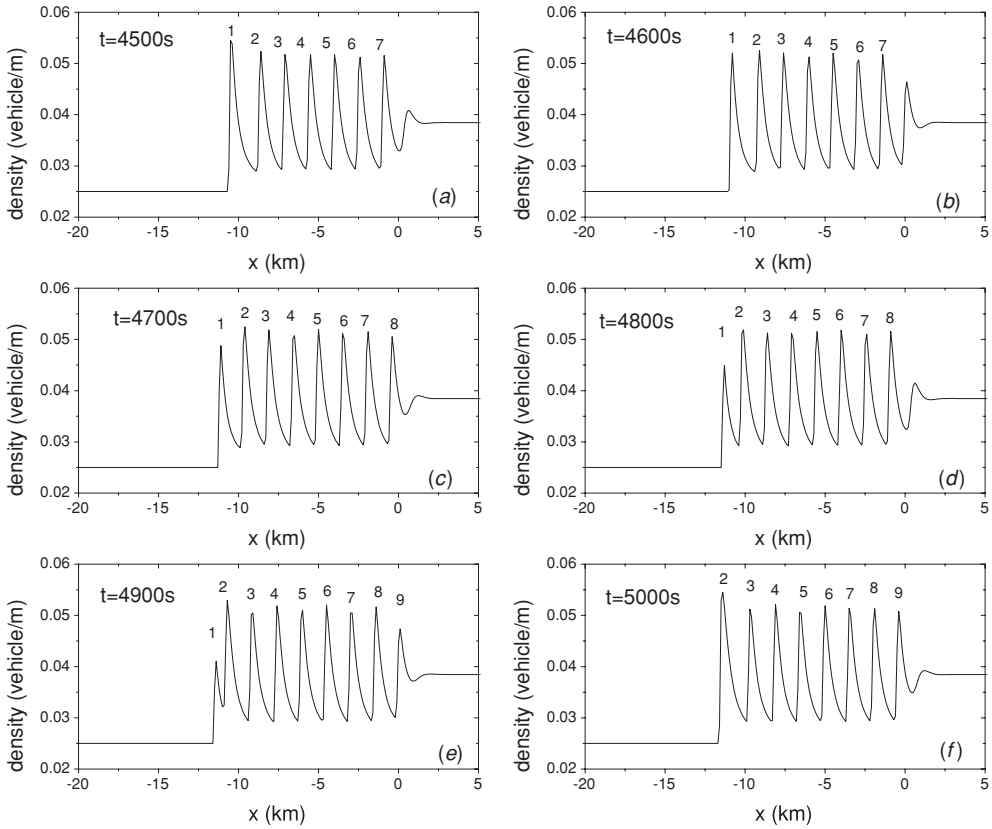


**Figure 6.** The dissolving and generating of the clusters in unstable traffic obtained at $k_u = 0.025$ vehicle $\mathrm{m}^{-1}$, $k_d = 0.038\,46$ vehicle $\mathrm{m}^{-1}$.

regions a, d, e and f shrink (figure 2(*c*)). Note that for $c_0 = 18$ m $\mathrm{s}^{-1}$, the oscillatory region b expands to the extent that regions e and a are separated by region b.

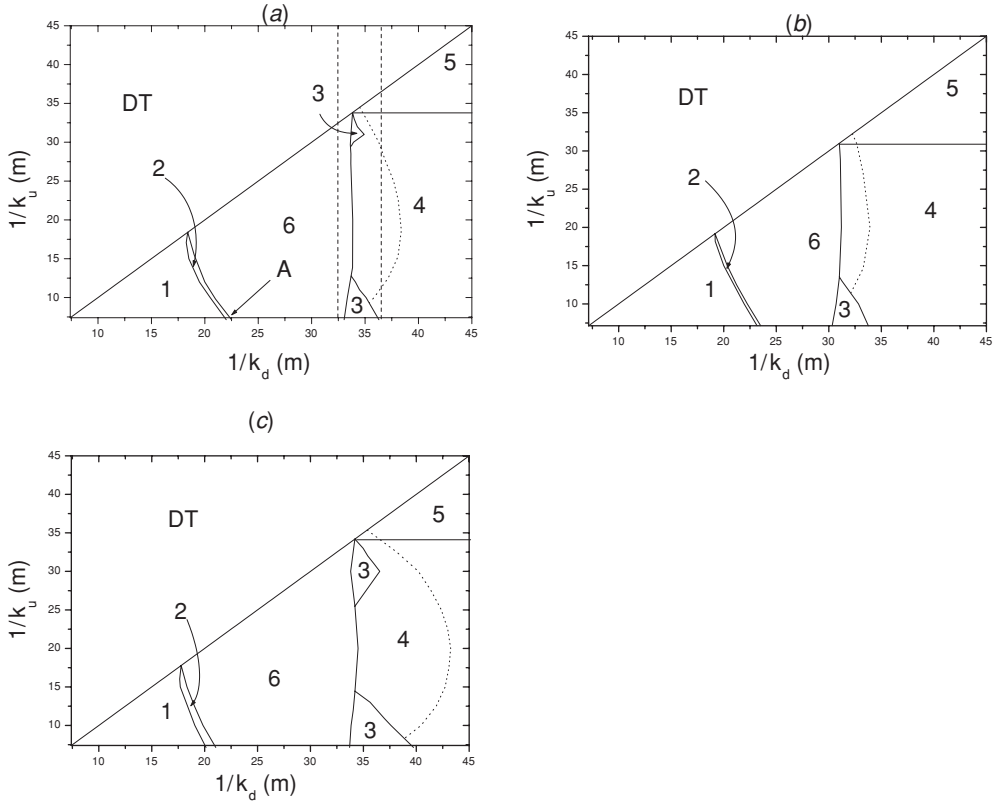


**Figure 7.** Transitions of the AT derived from the numerical simulations of the SG model at (*a*) $c_0 = 20$ m s$^{-1}$; (*b*) $c_0 = 22$ m s$^{-1}$; (*c*) $c_0 = 18$ m s$^{-1}$. In (*a*), the dashed lines represent the critical densities $k_{c1}$ and $k_{c2}$ from the right to the left.

## 4. Accelerating traffic

In this section, we concentrate on the AT, i.e. the transitions from high density into low density. First, we study the traffic patterns at $c_0 = 20$ m s$^{-1}$ and similar to the case of DT, the AT can be either stable or unstable. Nevertheless, different from the DT, the stable traffic of AT can only be classified into five categories. They are stationary acceleration wave (region 1), oscillatory (region 2), Bando wave and a second shock (region 3), Bando wave, plateau and dispersive tail (region 4) and purely dispersive (region 5) as shown in figure 7(*a*). The representative patterns of the five regions are shown in figure 8. For regions 3 and 4, the density first jumps from an upstream density $k_u$ to an intermediate density $k_b$, before it eventually matches the downstream density through a second shock (region 3) or dispersive tail (region 4). The jump from the upstream density $k_u$ to the intermediate density $k_b$ is also called the Bando wave, which is a stationary acceleration wave in the AT case. Furthermore, two points need to be noted. (i) Region 3 is composed of two separated parts. (ii) The oscillatory tail appears in the dispersive wave as shown in figure 9. The affected region is plotted to the left of the dotted line shown in figure 7.

As in the DT case, let us investigate the transitions between the unstable and the stable traffic in AT. Since the unstable region 6 borders three different stable regions 2, 3 and 4, we discuss each transition separately.

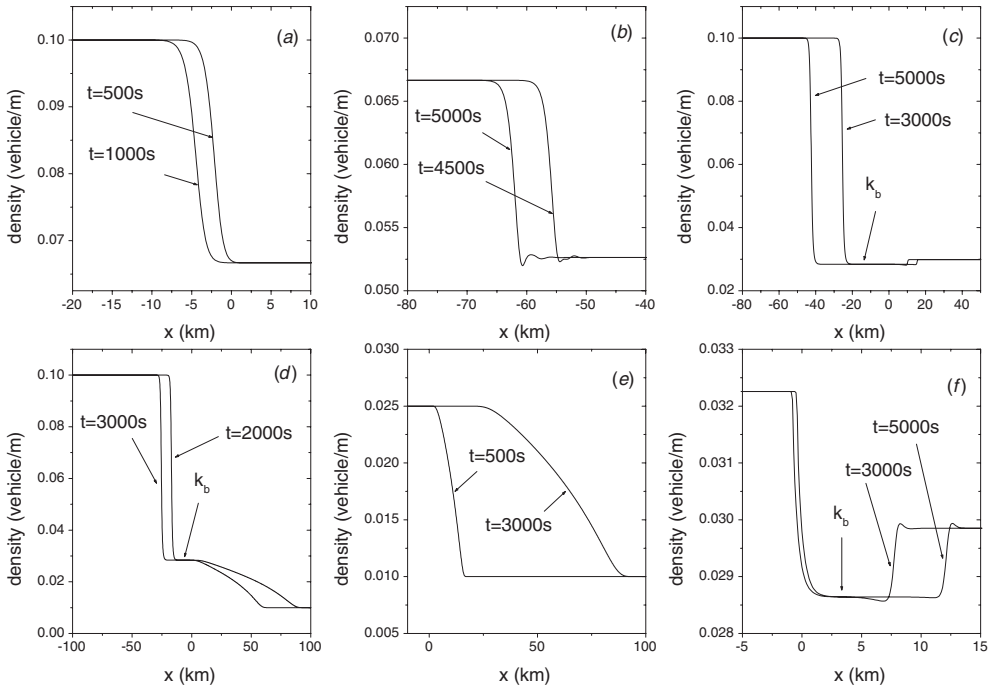


**Figure 8.** (*a*)–(*e*) are typical patterns of regions 1–5 in figure 7(*a*), and (*f*) is the typical pattern of the upper part of region 3 in figure 7(*a*). Here $k_u$ and $k_d$ are (*a*) 0.1, 0.066 67; (*b*) 0.066 67, 0.052 63; (*c*) 0.1, 0.029 85; (*d*) 0.1, 0.01; (*e*) 0.025, 0.01; (*f*) 0.032 26, 0.029 85 vehicle $\mathrm{m}^{-1}$.

First, we consider the transition between regions 3 and 6. If we fix the upstream density and merely change the downstream density near the boundary between regions 3 and 6, we can find that the Bando wave remains the same despite the stability of traffic and the instability actually originates from the new DT problem $(k_b, k_d)$. See the results presented in figure 10. If the DT problem $(k_b, k_d)$ is stable, then the AT problem $(k_u, k_d)$ falls into region 3 as shown in figure 10(*a*). If, however, the DT problem $(k_b, k_d)$ is unstable, then for the AT problem $(k_u, k_d)$, unstable traffic forms as shown in figure 10(*b*).

Secondly, we study the transition between the unstable region 6 and the oscillatory region 2. Note that in the unstable traffic region 6, given the same downstream density, if the upstream density increases to a certain value, then the instability disappears. For the purpose of explanation, we choose the following two typical downstream densities.

(i) $k_d = 0.051\,28$ vehicle $\mathrm{m}^{-1}$. For such a downstream density, the unstable traffic is characterized by the 'dipole-like' structure (figure 11(*a*)). Such a structure can be regarded as a single anti-cluster. The density of the outflow from the anti-cluster is $k_*$ and accordingly the flow rate $k_* u_e(k_*)$. With the increase of the upstream density, the upstream flow rate decreases. If the upstream flow rate decreases to a value less than the outflow rate $k_* u_e(k_*)$ from the anti-cluster, the anti-cluster cannot be maintained even if it forms. In this situation, oscillatory traffic exists instead of unstable traffic.

(ii) $k_d = 0.047\,62$ vehicle $\mathrm{m}^{-1}$. For such a downstream density, the unstable traffic is characterized by a complex sequence of anti-clusters (figure 11(*b*)). For this case, even if the upstream flow rate is less than the outflow rate from the anti-cluster, it does not always mean the traffic is stable because if the dissolving rate of the anti-cluster is not greater

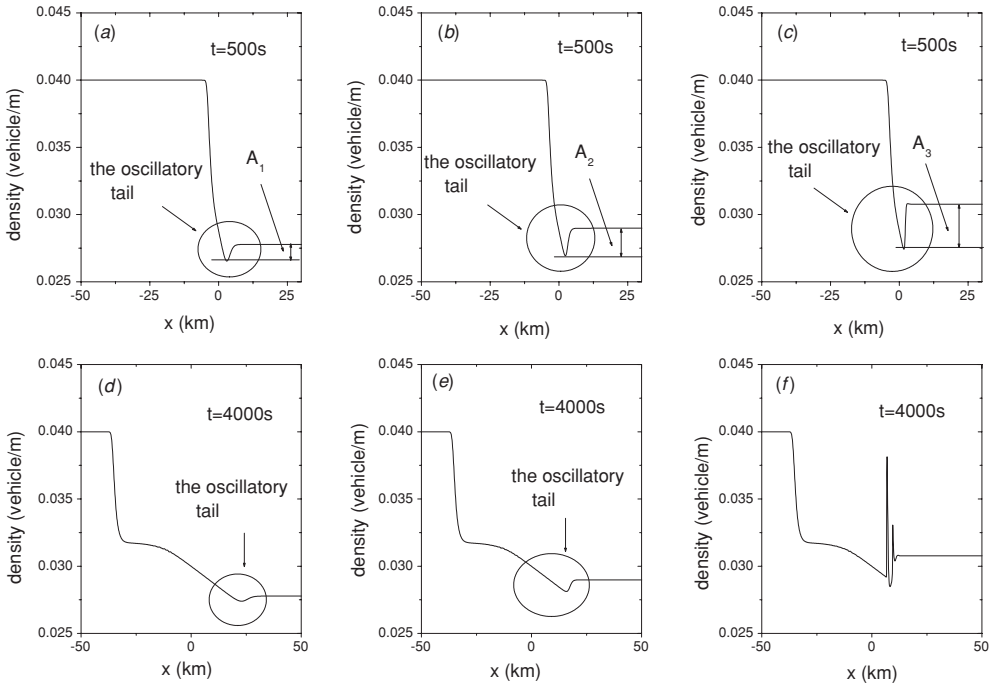


**Figure 9.** The traffic patterns nearby the boundary between regions 4 and 6 in figure 7(*a*). The upstream density is fixed at $k_u = 0.04$ vehicle m$^{-1}$. In (*a*), (*d*) $k_d = 0.027\,78$ vehicle m$^{-1}$; (*b*), (*e*) $k_d = 0.028\,98$ vehicle m$^{-1}$; (*c*), (*f*) $k_d = 0.030\,77$ vehicle m$^{-1}$. In (*a*)–(*c*), $A_1$, $A_2$, and $A_3$ denote the amplitude of the oscillatory tail and it is obvious that $A_1 < A_2 < A_3$.

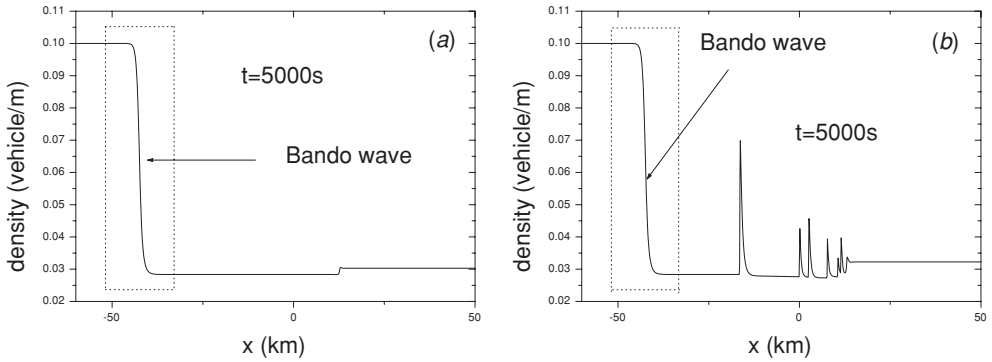


**Figure 10.** The two different traffic patterns nearby the boundary between regions 3 and 6 in figure 7(*a*). (*a*) $k_u = 0.1$ vehicle m$^{-1}$, $k_d = 0.0303$ vehicle m$^{-1}$, and the traffic pattern falls into region 3. (*b*) $k_u = 0.1$ vehicle m$^{-1}$, $k_d = 0.032\,26$ vehicle m$^{-1}$, and the traffic pattern falls into region 6.

than the generating rate of the anti-cluster, the anti-clusters can still be maintained. For example, see the results presented in figure 12. We number the anti-clusters in order to better understand the dissolving and generating of the anti-clusters. We can see that from 4750 to 5500 s, two anti-clusters 1 and 4 have dissolved and two anti-clusters 5 and 6 are generated. The pattern at 5500 s is almost unaltered compared with that in 4750 s.

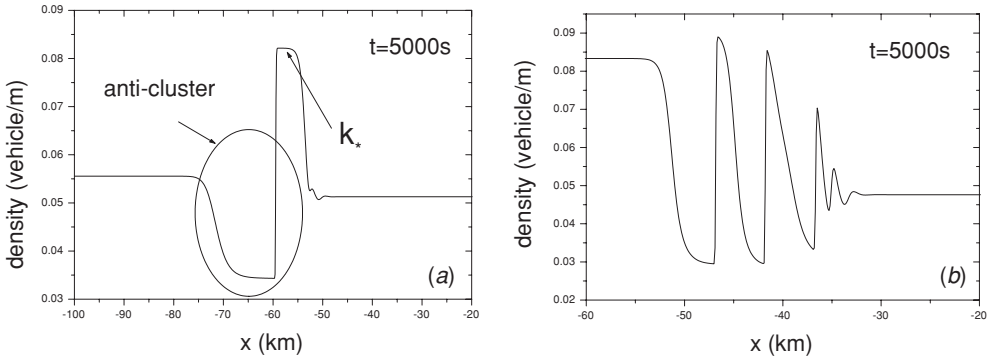


**Figure 11.** The different unstable traffic patterns of two typical downstream densities. (*a*) $k_u = 0.055\,56$ vehicle m$^{-1}$, $k_d = 0.051\,28$ vehicle m$^{-1}$, and the traffic pattern is characterized by a 'dipole-like' structure. (*b*) $k_u = 0.083\,33$ vehicle m$^{-1}$, $k_d = 0.047\,62$ vehicle m$^{-1}$, and the traffic pattern is characterized by a complex sequence of anti-clusters.

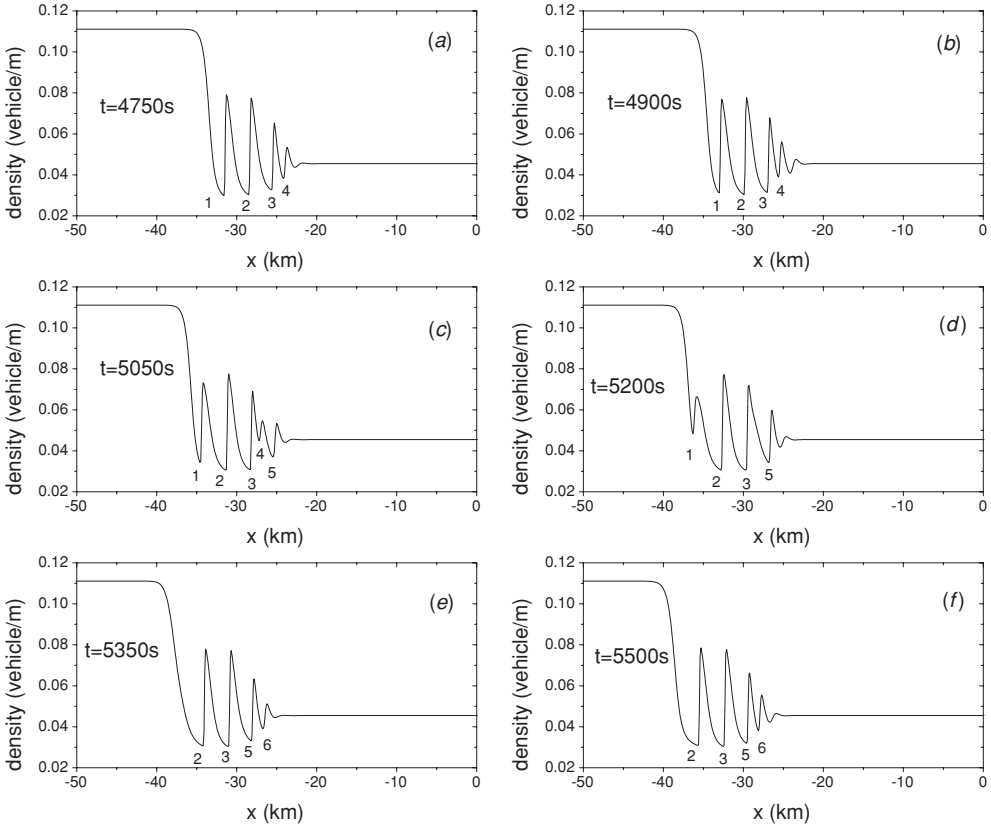


**Figure 12.** The dissolving and generating of the anti-clusters in the unstable traffic obtained at $k_u = 0.111\,11$ vehicle m$^{-1}$, $k_d = 0.045\,45$ vehicle m$^{-1}$.

In this way, the unstable traffic can be maintained. Only when the upstream flow rate is so small that the dissolving rate of the anti-cluster is greater than the generating rate may the unstable traffic disappear. Nevertheless, note that if $k_d$ is greater than the density

$k_A \approx 0.044\,49$ vehicle m$^{-1}$ of point A in figure 7($a$), even if the upstream reaches the jam density and zero flow, the dissolving rate of the anti-clusters is still less than the generating rate; thus, unstable flow always exists.

Therefore, we can draw a similar conclusion as in the DT case: the reason for the transition from region 6 to region 2 is the upstream flow rate, which is not large enough to maintain the unstable traffic.

Finally, we examine the transition between regions 6 and 4. The simulations show that if we fix the upstream density and merely increase the downstream density near the boundary between regions 6 and 4, the amplitude of the oscillatory tail increases accordingly (figures 9($a$)–($c$)). If the amplitude of the oscillation exceeds the critical amplitude, the oscillatory traffic will evolve into instability (figure 9($f$)). Otherwise, the stable pattern remains (figures 9($d$) and ($e$)).[2]

If we increase the value of $c_0$, the stability of the traffic flow is enhanced and accordingly the unstable region 6 shrinks. Meanwhile, regions 2 and 3 shrink as well. In contrast, regions 1, 4 and 5 expand (figure 7($b$)). Similarly, if we decrease $c_0$, regions 2, 3 and 6 expand and regions 1, 4 and 5 shrink (figure 7($c$)). Note that for $c_0 = 22$ m s$^{-1}$, region 3 shrinks to the extent that the upper part of region 3 disappears.

## 5. Conclusion

In this paper, we study the merging of a platoon of moving cars at one density into another platoon moving with a different density. We carry out simulations that involve instability. We find that both the DT and the AT can either be stable or unstable for different pairs of ($k_u$, $k_d$) and the stable traffic patterns can be further classified into five or six categories. Since the properties of the stable patterns are analogous to those discussed in [26], we only concentrate on the transitions between the unstable and the stable patterns in this paper.

The simulations show that if no Bando wave is involved, the reason for the transition from the unstable traffic pattern to the stable pattern is that the upstream flow rate is not large enough to maintain the unstable traffic in both the DT and AT problems. On the other hand, if the Bando wave is involved, the DT and AT problems show some difference.

- For a DT problem, it transfers into a Bando wave and a new AT problem with an upstream density $k_b$ and a downstream density $k_d$, and the stability of the original DT problem is determined by the new AT problem. In the new AT problem, no Bando wave is involved and thus the reason for the transition from the unstable traffic pattern to the stable pattern of the new AT problem is that the upstream flow rate $k_b u_e(k_b)$ is not large enough to maintain the unstable traffic, so the reason for the transition from the unstable traffic pattern to the stable pattern of the original DT problem is that the intermediate flow rate $k_b u_e(k_b)$ is not large enough to maintain the unstable traffic.
- For an AT problem, it transfers into a Bando wave and a new problem with an upstream density $k_b$ and a downstream density $k_d$, and the stability of the original AT problem is determined by the new problem ($k_b$, $k_d$).

[2] The SG model can reproduce the characteristic properties of the traffic flows formulated by Kerner and Konhäuser [33]. For densities $k < k_{c1}$, the traffic is stable with respect to localized perturbations and for a range $k_{c2} < k < k_{c3}$ of densities, it is linearly unstable. For the density regime $k_{c1} \leqslant k \leqslant k_{c2}$, it is metastable; i.e. it behaves nonlinearly unstable with respect to perturbations exceeding a certain critical amplitude, but otherwise stable. The simulation indicates that $k_{c1} = 0.027\,62$ vehicle m$^{-1}$, $k_{c2} = 0.030\,58$ vehicle m$^{-1}$ and $k_{c3} = 0.049\,90$ vehicle m$^{-1}$ for $c_0 = 20$ m s$^{-1}$.

- If $k_b < k_d$, then the new problem is a DT problem. In the new DT problem, no Bando wave is involved, and thus the reason for the transition from the unstable traffic pattern to the stable pattern of the new DT problem is that the upstream flow rate $k_b u_e(k_b)$ is not large enough to maintain the unstable traffic, so the reason for the transition from the unstable traffic pattern to the stable pattern of the original AT problem is that the intermediate flow rate $k_b u_e(k_b)$ is not large enough to maintain the unstable traffic.
- If $k_b > k_d$, then the new problem is still a AT problem and it is a dispersive tail. The transition from the unstable traffic pattern to the stable pattern of the original AT is determined by the amplitude of the oscillatory tail of the dispersive wave. If the amplitude exceeds the critical value, then the AT is unstable. Otherwise, it is stable.

## Acknowledgments

This study is supported by The National Natural Science Foundation of China (grant no 19872062).

## References

[1] Schreckenberg M and Wolf E D (ed) 1998 *Traffic and Granular Flow '97* (Berlin: Springer)
[2] Chowdhury D, Santen L and Schadschneider A 2000 *Phys. Rep.* **329** 199
[3] Gazis D C, Herman R and Rothery R W 1961 *Oper. Res.* **9** 545
[4] Bando M *et al* 1995 *Phys. Rev.* E **51** 1035
[5] Jiang R, Wu Q S and Zhu Z J 2001 *Phys. Rev.* E **64** 017101
[6] Treiber M, Hennecke A and Helbing D 2000 *Phys. Rev.* E **62** 1805
[7] Tomer E, Safonov L and Havlin S 2000 *Phys. Rev. Lett.* **84** 382
[8] Biham O, Middleton A A and Levine D A 1992 *Phys. Rev.* A **46** R6124
[9] Nagel K and Schreckenberg M 1992 *J. Physique* I **2** 2221
[10] Helbing D 1996 *Phys. Rev.* E **53** 2366
[11] Helbing D, Hennecke A, Shvetsov V and Treiber M 2001 *Transp. Res.* B **35** 183
[12] Prigogine I and Herman R 1971 *Kinetic Theory of Vehicular Traffic* (New York: Elsevier)
[13] Lighthill M J and Whitham G B 1955 *Proc. R. Soc.* A **229** 317
[14] Richards P I 1956 *Oper. Res.* **4** 42
[15] Payne H J 1971 *Mathematical Models of Public Systems* vol 1 ed G A Bekey (La Jolla, CA: Simulation Council)
[16] Liu G Q, Lyrintzis A S and Michalopoulos P G 1998 *Transp. Res. Rec.* **1644** 37
[17] Zhang H M 1998 *Transp. Res.* B **32** 485
[18] AW A and Rascle M 2000 *SIAM J. Appl. Math.* **60** 916
[19] Jiang R, Wu Q S and Zhu Z J 2002 *Transp. Res.* B **36** 405
[20] Jiang R, Wu Q S and Zhu Z J 2001 *Chin. Sci. Bull.* **46** 345
[21] Lee H Y, Lee H W and Kim D 1999 *Phys. Rev.* E **59** 5101
[22] Helbing D, Hennecke A and Treiber M 1999 *Phys. Rev. Lett.* **82** 4360
[23] Daganzo C F, Cassidy M J and Bertini R L 1999 *Transp. Res.* A **33** 365
[24] Kerner B S and Rehborn H 1996 *Phys. Rev.* E **53** R1297
[25] Kerner B S and Rehborn H 1996 *Phys. Rev.* E **53** R4275
[26] Berg P and Woods A 2001 *Phys. Rev.* E **63** 036107
[27] Daganzo C F 1995 *Transp. Res.* B **29** 277
[28] Leveque R J and Yee H C 1990 *J. Comput. Phys.* **86** 187
[29] Harten A, Lax P D and Van Leer B 1983 *SIAM Rev.* **25** 35
[30] Einfeldt B *et al* 1991 *J. Comput. Phys.* **92** 273
[31] Kurtze D A and Hong D C 1995 *Phys. Rev.* E **52** 218
[32] Komatsu T S and Sasa S 1995 *Phys. Rev.* E **52** 5574
[33] Kerner B S and Konhäuser P 1994 *Phys. Rev.* E **50** 54